

# THE ELECTROTHERMAL MACROMODEL OF ZCS RESONANT CONVERTER CONTROLLERS FOR SPICE

Krzysztof Górecki, Janusz Zarębski

Gdynia Maritime University, Department of Marine Electronics

**Key words:** ZCS converter controllers, SPICE, electrothermal macromodels

**Abstract:** The main aim of this paper is to propose a new electrothermal (including selfheating) macromodel of the MC34066 ZCS resonant converter controller for SPICE. The macromodel structure results both from the controller block diagram presented by the producer in the catalogue data and the principle of its operation. This macromodel formed in the network form describes the fundamental and the most important features of the considered IC. The proposed macromodel was verified experimentally. The majority of the macromodel parameter values have been obtained from the measured characteristics.

## SPICE elektrotermični model ZCS resonančnih pretvornikov

**Ključne besede:** ZCS pretvornik, SPICE, elektrotermični model

**Izveček:** V prispevku predlagamo nov SPICE elektrotermični model za MC34066 ZCS resonančni pretvornik. Makromodel je nastal na osnovi blok diagrama proizvajalca, kakor tudi na osnovi principa delovanja. Makromodel v obliki blok vezja opiše najbolj pomembne lastnosti integriranega vezja. Predlagani model smo preverili tudi eksperimentalno. Večino parametrov makromodela smo določili na osnovi merjenih karakteristik

### 1. Introduction

The resonant converters switching at zero voltage (ZVS) or at zero current (ZCS) /1, 2, 3/ are more and more popular circuits which belong to the class of Switch Mode Power Supplies (SMPS).

In the process of designing such a class of converters, fully credible models describing the converter components (diodes, transistors, etc.), or describing the whole circuit, play a fundamental role and the proper computer tools are necessary as well. Today, SPICE along with the built-in models and worked out by the producers macromodels of some devices such as: diodes, transistors, inductors, transformers and the large class of ICs is such a convenient tool. For example, the macromodels of controllers dedicated to dc-dc converters are available in the SWIT\_REG.LIB library /4/ and in the libraries attached to the Basso book /5/. Unfortunately, there are no models or macromodels of resonant converter controllers available for SPICE users. The preliminary versions of ZVS and ZCS converter controller macromodels elaborated earlier by the authors can be found in the papers /6, 7/. The macromodels, presented in the cited papers are the isothermal ones and in these macromodels selfheating in semiconductor devices is omitted.

Due to the selfheating existing in IC, the electrical power is changed into heat, which in the non-ideal conditions of heat removing to the surrounding results in an increase of the inner temperature  $T_j$ . In turn, due to an increase of the device inner temperature both a change of d.c. characteristics and a decrease of device reliability are observed /8, 9/.

To include the selfheating phenomena in the computer-aided design and the analysis of SMPS the special kind of models, called the electrothermal ones should be used.

In the literature the electrothermal models of semiconductor devices for SPICE, e.g. /10, 11, 12/ are proposed, but there is no information about electrothermal models of monolithic integrated circuits.

The aim of the paper is to present a new electrothermal macromodel of the MC34066 controller dedicated for SPICE. In the macromodel construction process the modelling idea, used by the authors for the first time in the case of PWM controller electrothermal macromodel formulation /13/, has been adopted.

The monolithic controller MC34066 made by ON Semiconductor is dedicated for the class of resonant ZCS switched mode power supplies. By means of this controller the frequency modulation of the output signal is realised.

The considered controller can operate with the constant or variable value of the pulse duration time (on-time or off-time mode). The combination of both the modes of operation is also possible /14/.

At the outputs of MC34066 one can get two signals of the frequency from 40 kHz to 1.2 MHz and the high value of the current efficiency.

According to the catalogue data /14/ the output frequency signals can be changed a thousand times, and the frequency band of the error amplifier is equal to 5 MHz. The under-

voltage and overcurrent protection, as well as the soft-starting circuit, are included in the considered IC.

The time duration of the high level at the generator output as well as the maximum value of the output signal period are determined by the external RC elements. The value of the output signal period depends on the voltage existing at the output of the error amplifier.

In Chapter 3, the proposed macromodel form of the MC34066 controller is shown and described, whereas Chapter 4 presents the results of the measurements and calculations of two important parameters, such as the pulse time duration and the period of the output signals of the considered controller working in the special test circuit with different values of the external RC elements.

### 3. The Macromodel Structure

The macromodel structure results from the controller block diagram presented by the producer in the catalogue data /9/, the principle of operation of the controller of the ZCS converter as well as the roles of formulating the device electrothermal models /15/. This macromodel, presented in Fig.1 in the network form, describes the fundamental and the most important features of the considered IC. The efficiencies of the controlled sources are given both as the logic expressions resulting from the IC structure and as the functions formulated on the measurement data.

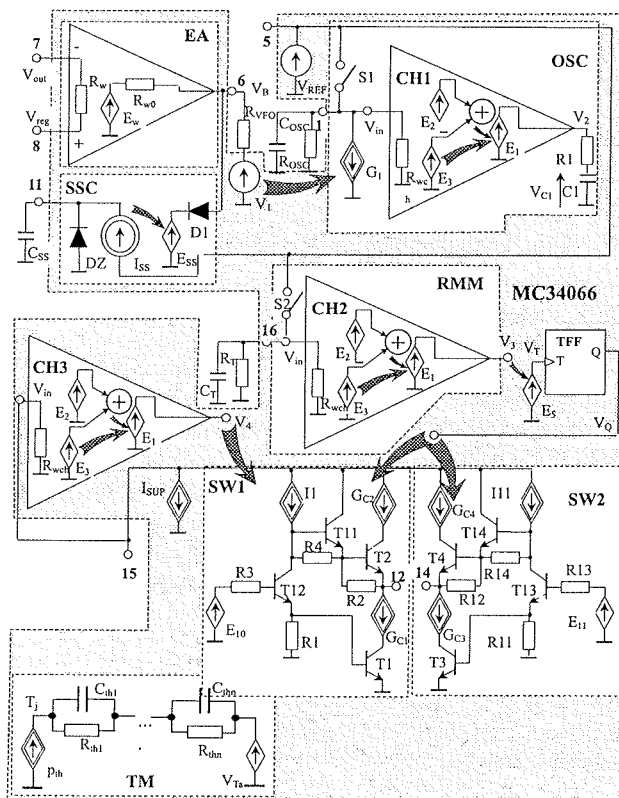


Fig.1. The macromodel diagram of the ZCS controller

Ten essential blocks: reference voltage source ( $V_{REF}$ ), error amplifier (EA), oscillator (OSC), retrigerrable monostable multivibrator (RMM), T flip-flop (TFF), soft-start circuit (SS), under-voltage protection (CH3), two identical output stages (SW1 and SW2) and the thermal model (TM) can be distinguished in the macromodel.

The error amplifier is described as a quasi-ideal operation amplifier in which the efficiency of the voltage control source  $E_w$  given by

$$E_w = K_u \cdot (V_{reg} - V_{out}) \quad (1)$$

is proportional to the open loop amplification factor ( $K_u$ ) and the amplifier differential input voltage ( $V_{reg} - V_{out}$ ), whereas  $R_w$  and  $R_{w0}$  represent the input and output amplifier resistances, respectively.

As it is seen from Fig.2, the inputs of the considered error amplifier are excited by the control voltage ( $V_{reg}$ ) and the feedback voltage  $V_{out}$ , respectively. Its output controls the discharging current of the auxiliary capacitor  $C_{osc}$ .

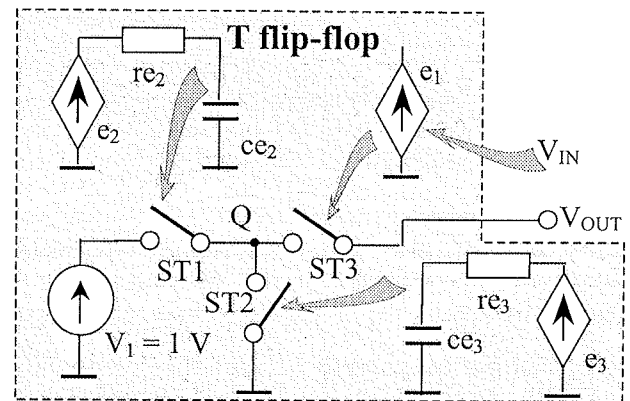


Fig.2. The network representation of the T flip-flop circuit

In the macromodel the typical catalogue values of the parameters  $R_w = 5 \text{ M}\Omega$ ,  $R_{w0} = 75 \Omega$ , and  $K_u = 10^5$  have been taken into account.

The two-terminal network consisting of the resistor  $R_T$  and the capacitor  $C_T$  is used for programming the pulse time duration. In turn, the second two-terminal network composed of  $C_{osc}$  capacitor and  $R_{osc}$  resistor determines the minimum oscillation frequency, whereas the main task of the current source of the efficiency  $G_1$  controlled by voltage  $V_B$ , is to discharge  $C_{osc}$  capacitance. The efficiency of this source is described by

$$G_1 = \text{LIMIT} \left( \frac{V_B - V_1 \cdot (1 - a_T \cdot (T - T_0))}{R_{VFO}}, \frac{V_2}{R_{VFO}}, \frac{V_3}{R_{VFO}} \right) \quad (2)$$

where LIMIT denotes the built-in function of SPICE,  $T$  is the temperature,  $V_1, V_2, V_3, a_T$  are the model parameters, and  $T_0$  is the reference temperature, at which parameter values have been estimated.

Two switches – S1 and S2 controlled by the signal existing at the output of the comparator with hysteresis (CH1) are switched on when the value of the voltage across  $C_{OSC}$  capacitance decreases below 3.6 V. On the contrary, they are switched off in the case when this voltage increases up to 5.1 V.

The comparator with hysteresis is modelled by means of three voltage controlled sources  $E_1$ ,  $E_2$ ,  $E_3$  of the efficiencies given by /16/

$$E_1 = LIMIT(x,1,0) \quad (3)$$

where: LIMIT denotes the standard SPICE function and x is given by

$$x = \begin{cases} E2 & \text{for } V_{in} < V_{min} \text{ and } V_{in} > V_{max} \\ E2 + E3 & \text{for } V_{min} < V_{in} < V_{max} \end{cases} \quad (4)$$

$$E2 = \begin{cases} 1 & \text{for } V_{in} < V_{min} \\ \frac{1}{V_{mx} - V_{min}} \cdot (V_{in} - V_{min}) & \text{for } V_{min} < V_{in} < V_{mx} \\ 0 & \text{for } V_{in} > V_{mx} \end{cases} \quad (5)$$

$$E3 = \begin{cases} 0 & \text{for } dV_{in}/dt < 0 \\ dV_{in}/dt & \text{for } 0 < dV_{in}/dt < 1 \\ 1 & \text{for } dV_{in}/dt > 1 \end{cases} \quad (6)$$

where  $V_{min}$  and  $V_{max}$  denote the values of the bottom and the upper boundary of the hysteresis loop. In the model  $V_{min} = 3.5$  V,  $V_{mx} = 3.51$  V and  $V_{max} = 4.9$  V were assumed.

The input of the T flip-flop circuit (TFF) is controlled by the logic sum of the output signals of both the comparators. In turn, the output of the flip-flop circuit controls the output block consisting of two BJTs, operating in the emitter follower circuits.

The efficiency of the source  $E_5$  is

$$E_5 = LIMIT(V_2 + V_3,1,0) \quad (7)$$

where  $V_2$  and  $V_3$  denote the voltages at the outputs of the comparators CH1 and CH2, respectively.

In the soft-start circuit (SSC) the current source  $I_{SS}$ , whose efficiency is described by a Heaviside's jump of the value equal to  $9 \mu A / 9 /$ , charges the auxiliary capacitor  $C_{SS}$ . The Zener diode DZ limits the voltage on this capacitor to 3 V. The efficiency of the controlled voltage source  $E_{SS}$  is equal to the voltage on the capacitor  $C_{SS}$ . Because of the use of the diode D1, the slew rate of the error amplifier (EA), after switching on the power supply, is limited by the slew rate of  $C_{SS}$  capacitor voltage and the controller starts working with the minimum switching frequency.

The undervoltage lockout is realised by the use of the comparator with hysteresis CH3. If the supply voltage of control-

ler decreases under 9 V, the comparator output voltage  $V_4$  decreases to a low stage. The change of this voltage to a high stage requires an increase of the supply voltage to 16 V. The low stage of the output of the considered block causes the low stage on both the outputs of the MC34066 controller.

The output stage consists of two identical blocks: SW1 and SW2. In turn, each of them is composed of four bipolar transistors (BJT), four resistors and one current source. The shunt resistors are connected parallelly to BJT's base-to-emitter junctions in order to accelerate the transistors switching-off process /1/.

The bipolar transistors are described by their SPICE built-in model. The value of the series collector resistance is estimated according to the rate of the transistors switching-on.

The controlled current sources  $G_{C1}$ ,  $G_{C2}$ ,  $G_{C3}$  and  $G_{C4}$  model the temperature dependence of the collector resistance of the transistors T1, T2, T3, T4 operating in the output stage. These sources are described by the formulae

$$G_{Ci} = \frac{V_{GCI}}{R_C \cdot \alpha_{RC} \cdot (T - T_0)} \quad (8)$$

where  $i = 1, 2, 3, 4$ ,  $V_{GCI}$  is the voltage on the  $i$ -th source,  $R_C$  is the collector series resistance for  $T = T_0$ , whereas  $\alpha_{RC}$  denotes the temperature coefficient of  $R_C$  resistance.

The efficiency of two voltage sources  $E_{10}$  and  $E_{11}$  controlling the output stages depends on the input  $V_T$  and output  $V_Q$  voltages of T flip-flop. The considered sources are described by

$$E_{10} = (1 - V_Q) \cdot (1 - V_T) \cdot V_{CC} \quad (9)$$

$$E_{11} = V_Q \cdot (1 - V_T) \cdot V_{CC} \quad (10)$$

where  $V_{CC}$  denotes the supply voltage of the controller.

The efficiency of  $I_{SUP1}$  current source describes the current value consumed by the controller (without the output stage) from the source of the supply voltage. The obtained from the measurements values of  $I_{SUP1}$  are equal to 22.1 mA.

The pulse time duration both at the controller output and the output of the flip-flop are equal to each other. The flip-flop is modelled by means of the circuit shown in Fig.2.

The voltage controlled sources  $e_1$ ,  $e_2$  and  $e_3$  are of the efficiency equal 0 or 1, depending on the logic state at the input ( $V_{IN}$ ) and the output ( $V_{OUT}$ ) of the flip-flop. The essential role of the resistances  $re_2$ ,  $re_3$  and capacitances  $ce_2$ ,  $ce_3$  is to delay properly the signals controlling switches S1 and S2 in such a way which ensures that both the switches are not switched on at the same time.

The efficiency of the source  $e_2$  equals 1, when at the input (output) of the flip-flop the signal increases (low state) or when at its input (output) the voltage is constant (high state).

In turn, the efficiency of the source  $e_3$ , similarly to what was described above, is equal to 1 when at the input (output) of the flip-flop the signal increases (high state exists) or when at its input (output) the voltage is constant (low state exists).

The switch ST1 is switched on when the voltage at the capacitance  $ce_2$  is greater than 0.5 V, whereas the switch ST2 is switched on when the voltage across the capacitance  $ce_3$  is greater than 0.5 V. The switch ST3 is switched on while the control signal is increasing, otherwise it is switched off.

The thermal model (TM) consists of the controlled current source  $p_{th}$  of the efficiency equal to the dissipated power in the controller, the RC network, representing the transient thermal impedance of the controller and independent voltage source  $V_{Ta}$ , whose efficiency corresponds to the ambient temperature. The efficiency of the  $p_{th}$  source is given by

$$p_{th} = V_{CC} \cdot I_{SUP1} + \sum_{i=1}^4 i_{Ci} \cdot v_{CEi} \quad (11)$$

where  $i_{Ci}$  and  $v_{CEi}$  denote the collector current and the collector-to-emitter voltage of the transistor  $Ti$  ( $i = 1, 2, 3, 4$ ), respectively.

#### 4. Verification of the Macromodel

The proposed macromodel has been verified experimentally. For the investigated device (MC34066) the test circuit (TC) with the resistance load and without a feedback loop has been proposed by the authors (Fig.3). Some measurements for the various values of the ambient temperature, supply voltage, and the load resistance as well as for some values of RC elements connected to the oscillator terminals and determining the period and the dead time of the output signals have been performed in TC.

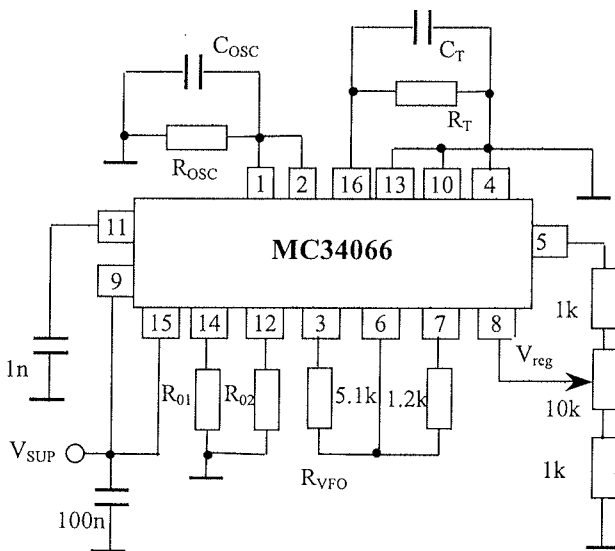


Fig.3. The test circuit

As an example, in Fig.4 the results of the simulations (lines) and measurements (squares) of the period of the output signal  $T_S$  on the regulation voltage  $V_{reg}$  for two values of temperature and different values of external RC elements are presented. In both cases the identical values of  $R_{OSC} = 89.45 \text{ k}\Omega$  and  $R_T = 14.86 \text{ k}\Omega$  are used, whereas the other elements are of the following values:

- a) for the case presented in Fig.5a:  $C_{OSC} = 101.8 \text{ pF}$ ,  $C_T = 105,4 \text{ pF}$ ,  $V_{SUP} = 20 \text{ V}$  and  $R_0 = 1.2 \text{ k}\Omega$ ,
- b) for the case presented in Fig.5b:  $C_{OSC} = 327 \text{ pF}$ ,  $C_T = 268.8 \text{ pF}$ ,  $V_{SUP} = 12 \text{ V}$  and  $R_0 = 208 \Omega$ .

As seen from Fig.4, a satisfactory agreement between the calculations and measurements of the dependencies of the period of the output signal on the regulation voltage, for both the temperatures, has been achieved. It is worth noticing that the period time decreases nearly tenfold in the range of the regulation. Increasing the temperature pushed the characteristics to the left direction, which is especially important in the range of  $V_{reg}$  changing from 1.2 V to 2 V, where the values of  $T_S$  corresponding to the selected value of  $V_{reg}$  can differ from each other by over 30%.

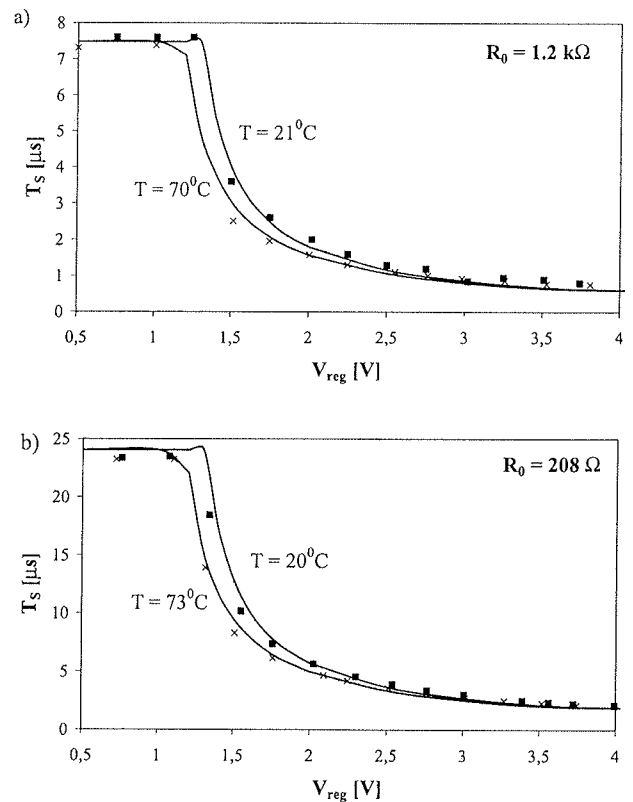


Fig.4. Calculated (lines) and measured (squares) dependencies of the period time on the regulation voltage

The shape of the obtained characteristics qualitatively agrees with the results corresponding to the other values of RC elements, which confirms the correctness of the proposed model.

In turn, in Fig.5, the results of the measurements and simulations of MC34066 operating in the test circuit (Fig.4) for the changed values of the external elements, which are  $C_{OSC} = 327$  pF,  $C_T = 268.8$  pF,  $R_0 = 208 \Omega$  and for two temperatures  $T_1 = 20^\circ\text{C}$  and  $T_2 = 73^\circ\text{C}$  are presented.

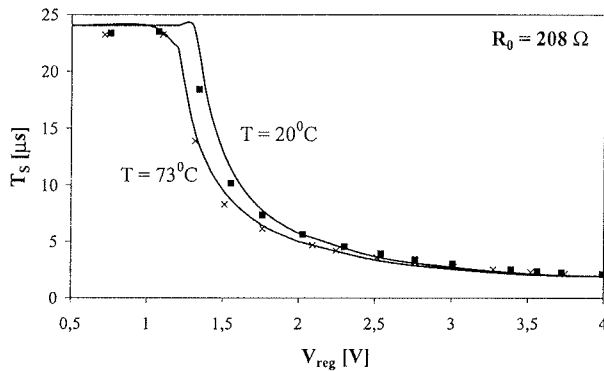


Fig.5. Measured and calculated dependence of  $T_s$  on  $V_{reg}$

As seen, also in this case a good agreement between the calculation and measurement results for both the temperatures in the whole range of the regulation voltage  $V_{reg}$ , was achieved. The shape of the obtained characteristics qualitatively agrees with the results corresponding to the other values of RC elements, which confirms the correctness of the proposed model.

In Fig.6 the measured and calculated dependences of the supply current  $I_{SUP}$  on the control voltage  $V_{reg}$  at fixed values of the supply voltage  $V_{CC}$  and the load resistance  $R_0$  are presented. The investigations have been performed for the following values of the external elements:  $C_{OSC} = 330$  pF,  $R_{OSC} = 91$  kW,  $C_T = 270$  pF,  $R_T = 14$  kW,  $T = 20^\circ\text{C}$ .

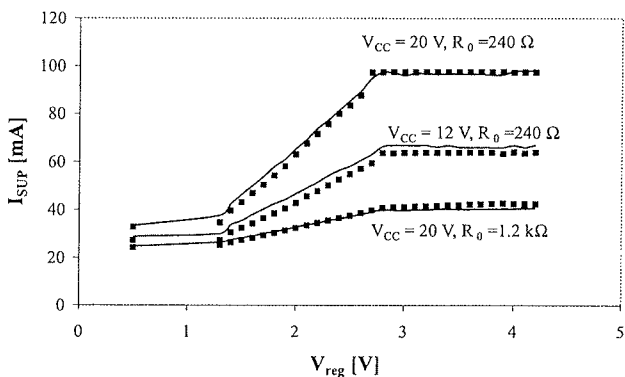


Fig.6. The dependence of the controller supply current on the regulation voltage

As seen, the results of the measurements and calculations fit very well.

From the dependences illustrated in Fig.6 it appears that  $I_{SUP}$  current value depends strongly on the  $V_{CC}$  and  $R_0$  values. Decreasing  $R_0$  and increasing  $V_{CC}$  cause the  $I_{SUP}$  to increase. On the other hand, the biggest value of  $I_{SUP}$  corresponds to the biggest values of  $V_{reg}$ , that is for the highest

frequencies of the control signal.  $I_{SUP}$  increases linearly in the range of  $V_{reg}$  changing from 1.3 V to 2.7V. So, this is the range in which the pulse time duration  $t_w$  and period  $T_s$  keep constant values.

Fig.7 illustrates the mode of operation of the soft-start block for  $C_{SS} = 1$  nF,  $C_{OSC} = 327$  pF,  $C_T = 268.8$  pF,  $R_{OSC} = 89.45$  kW,  $R_T = 14.86$  kW,  $V_{CC} = 12$  V and  $R_0 = 208 \Omega$ . In the figure, solid and dashed lines denote the simulation results of the considered controller obtained with the soft-start circuit taken into account and without it, respectively.

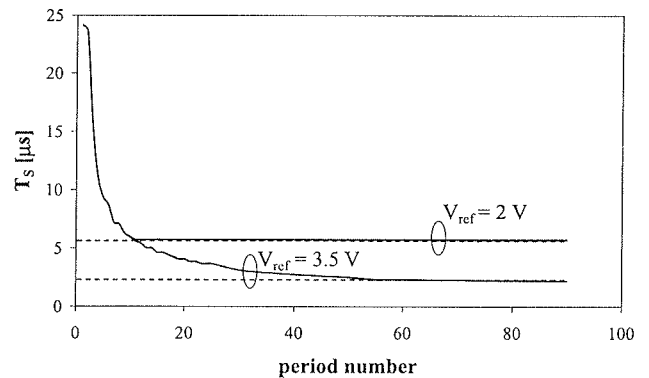


Fig.7. The dependence of the interval between two successive pulses on the period number

As seen, at the steady-state the values of  $T_s$  period corresponding to both the considered situations are practically the same, whereas immediately after the controller switching-on the soft-start circuit causes the interval between two successive pulses of the output signal to lengthen even tenfold. Such properties of the investigated controller are convenient for the principle MC34066 operation available in the catalogue data /14/.

In Fig.8 the calculated dependence of the device inner temperature on the voltage  $V_{reg}$  corresponding to the characteristics from Fig.7, is presented. As seen, the inner temperature depends on the supply voltage and the load resistance. For the maximum allowable value of  $V_{CC}$  and at  $R_0 = 240 \Omega$  the inner temperature tends to its maximum value given in the catalogue.

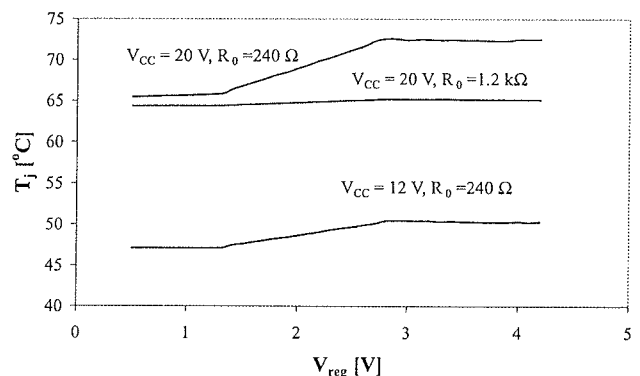


Fig.8. The calculated dependence of the inner temperature on the regulation voltage

## 5. Conclusions

In the paper the new electrothermal macromodel of ZCS controller dedicated for PSPICE is proposed. The basis for this macromodel preparation were the measurements of MC34066 characteristics. The macromodel has been verified experimentally in the test circuit worked out by the authors.

The model presented in Chapter 4 assures a good agreement with experimental results in the wide range of temperatures, the supply voltage, the load resistance, as well as the external RC elements. It is worth mentioning that this agreement is achieved both for on-time and off-time modes of MC34066.

- /1/ N. Mohan, T.M. Undeland, W.P. Robbins, *Power Electronics: Converters, Applications, and Design* (New York, John Wiley & Sons, 1995).
- /2/ M. Kazimierczuk, D. Czarkowski, *Resonant Power Converters* (New York, Wiley&Sons, 1995).
- /3/ R.W. Ericson, D. Maksimovic, *Fundamentals of Power Electronics* (Norwell, Kluwer Academic Publisher, 2001).
- /4/ Switch-reg.lib, *SPICE library*, 1998.
- /5/ Ch.P. Basso, *Switch-Mode Power Supply SPICE Cookbook* (New York, McGraw-Hill, 2001).
- /6/ K. Górecki, J. Zarębski, A New SPICE Macromodel of ZVS Resonant Converter Controller. *6th International Seminar on Power Semiconductors ISPS'2002*, Prague, 2002, pp. 195-198.
- /7/ K. Górecki, J. Zarębski, The SPICE Macromodel of MC34066 Controller. *6th International Conference on Unconventional Electromechanical and Electrical Systems UEES'04*, Alush-ta, 2004, Vol. 2, pp. 525-530.
- /8/ Speakman Z.: A model for the failure of bipolar silicon integrated circuits subjected to electrostatic discharge. *12th Annual Proceedings Reliability Physics*, 1974, p. 60.
- /9/ Stojadinovic N.: Failure physics of integrated circuits. A review. *Microelectronics and Reliability*, 1983, Vo. 23, No. 4, p. 609.
- /10/ J. Bielefeld, G. Pelz, H.B. Abel, G. Zimmer, "Dynamic SPICE-Simulation of the Electrothermal Behavior of SOI MOSFET's", *IEEE Transactions on Electron Devices*, Vol.42, No.11, 1995, pp.1968-1974.
- /11/ Chih-Ju Hung, P. Roblin, S. Akhtar, "Distributed B-spline electrothermal models of thyristors proposed for circuit simulation of power electronics". *IEEE Transactions on Electron Devices*, Vol.48, No.2, 2001, pp.353-366.
- /12/ Schurack E., Latzel T., Rupp W., Gotwald A.: Nonlinear Effects in Transistors Caused by Thermal Power Feedback : Simulation and Modeling in SPICE. *IEEE Int. Symp. on Circuits and Systems - ISCAS'92*, San Diego 1992, p. 879.
- /13/ J. Zarębski, K. Górecki, SPICE Modelling of PWM Controllers. *IEEE International Power Electronics Congress CIEP'2002*, Guadalajara, 2002, 2001, pp. 61-65.
- /14/ MC34066, MC33066 High Performance Resonant Mode Controllers. *Catalogue data, ON Semiconductor*, 2000.
- /15/ J. Zarębski, Modelling, Simulations and Measurements of Electrothermal Characteristics in Semiconductor Devices and Electronic Circuits. *Proceedings of Gdynia Maritime Academy*, Gdynia, 1996 (in Polish).
- /16/ K. Górecki, J. Zarębski, K. Posobkiewicz, The Electrothermal Macromodel of the Monolithic Voltage Regulator LT1073 for SPICE. *10th IEEE International Conference on Electronics, Circuits and Systems ICECS 2003*, Sharjah, 2003, pp. 1113-1116.

Dr. Krzysztof Górecki  
Prof. Janusz Zarębski  
Gdynia Maritime University  
Department of Marine Electronics  
Morska 83, 81-225 Gdynia, POLAND,  
Tel. ++48 58 6901448, ++48 58 6901599, fax ++48  
58 6217353  
E-mail: gorecki@am.gdynia.pl, zarebski@am.gdynia.pl

*Prispelo (Arrived): 07. 10. 2005; Sprejeto (Accepted): 30. 01. 2006*